Received: 2 January 2017 | Revised: 14 June 2017 | Accepted: 5 July 2017

DOI: 10.1002/cm.21387

RESEARCH ARTICLE

MAPK-15 is a ciliary protein required for PKD-2 localization and male mating behavior in *Caenorhabditis elegans*

Brian P. Piasecki[1] | **Thomas A. Sasani**[1,2] | **Alexander T. Lessenger**[1] | **Nicholas Huth**[1] | **Shane Farrell**[1]

[1]Department of Biology, Lawrence University, Appleton, Wisconsin

[2]Department of Human Genetics, University of Utah, Salt Lake City, Utah

Correspondence
Brian P. Piasecki, Department of Biology, Lawrence University, 711 E Boldt Way, Appleton, WI 54911.
Email: brian.p.piasecki@lawrence.edu

Funding information
National Science Foundation Major Research Instrumentation, Grant/Award Number: 1126711

Cilia are conserved cellular structures that facilitate sensory-based processes, including those required for neuronal and kidney functions. Here, we show that the human mitogen activated kinase-15 (MAPK-15) ortholog in *Caenorhabditis elegans* encodes a ciliary protein. A strain harboring a mutation in the catalytic site of the kinase domain results in ciliary-specific defects in tail neurons of both hermaphrodite and male worms, manifesting in dye uptake, dendrite extension, and male mating behavior defects. Transgenic-fusion constructs for two *mapk-15* isoforms (A and C) with full-length kinase domains were generated. Expression of either the A- or C-specific isoform rescues the dye-filling and male-mating defective phenotypes, confirming the ciliary function of *mapk-15*. Expression of *mapk-15* occurs in many ciliated-sensory neurons of the head and tail in hermaphrodite and male worms. Localization of MAPK-15 isoforms A and C occurs in the cell body, dendritic processes, and cilia. A *C. elegans* ortholog of polycystin-2, a protein that when defective in mammals results in autosomal dominant polycystic kidney disease, is mislocalized in the male ray neurons of *mapk-15* mutant worms. Expression of the *mapk-15* gene by the *pkd-2* promoter partially rescues the male-mating defects observed in *mapk-15* mutant animals. Expression of *mapk-15* is DAF-19/RFX dependent in some CSNs and DAF-19/RFX independent in others. Collectively, these data suggest that MAPK-15 functions upstream of PKD-2 localization to modulate ciliary sensory functions.

KEYWORDS
Caenorhabditis elegans, cilia, ciliated sensory neurons, mitogen activated kinase-15, polycystic kidney disease

1 | INTRODUCTION

Cilia are vital cellular structures that protrude from most non-dividing cells in the human body and facilitate a variety of sensory functions in tissues as disparate as the brain, lungs, and kidney (Satir and Christensen, 2008). Ciliary defects therefore result in several disorders, including autosomal dominant polycystic kidney disease (ADPKD), nephronophthisis (NPHP), and Bardet-Biedl syndrome (BBS; Hildebrandt, Benzing, & Katsanis, 2011). ADPKD affects more than one in every 1,000 individuals and is characterized by enlarged and cystic kidneys often resulting in late-stage renal failure in affected patients (Hildebrandt et al., 2011).

Polycystin-1 (PC1) and polycystin-2 (PC2) are proteins that localize to the cilia of kidney tubular epithelial cells and are deficient in patients affected by ADPKD (Pazour, San Agustin, Follit, Rosenbaum, & Witman, 2002; Yoder, Hou, & Guay, 2002). The genes *PKD1* and *PKD2* encode for the transmembrane receptor PC1 and calcium channel PC2 respectively that work alone or together to modulate the sensation of fluid flowing through kidney tubules (Bacallao and McNeill, 2009).

In healthy cells, PC1 and PC2 are translated into the ER membrane, transported through the endomembrane system, and are then either retained within the cilium or released from the cilium in extracellular vesicles (EVs; Pazour and Bloodgood, 2008; Wang and Barr, 2016). PC1 and PC2 each contain a unique targeting sequence that direct them through the trans-Golgi network to the ciliary base,

Abbreviations: ADPKD, autosomal polycystic kidney disease; CSNs, ciliated-sensory neurons; CFP, cyan fluorescent protein; GFP, green fluorescent protein; EVs, extracellular vesicles; MAPK15/MAPK-15, mitogen activated kinase-15; PC1/PKD-1, polycystin-1; PC2/PKD-2, polycystin-2; RFX, regulatory factor X; PCMC, periciliary membrane compartment.

through a process requiring membrane modifying small GTPases, IFT20, and several BBSome components (Follit et al., 2008; Geng et al., 2006; Kim et al., 2014; Scheffers et al., 2002; Su et al., 2014; Ward et al., 2011; Xu et al., 2015). Recently, sensory cilia have been shown to release EVs into their environment (Wang et al., 2014; Wood, Huang, Diener, & Rosenbaum, 2013), and EV cargos from renal cells contain ciliary proteins involved in kidney-related pathologies (Hogan et al., 2009; Pisitkun, Shen, & Knepper, 2004]. Trafficking defects of PC1 and PC2 likely underlie ADPKD pathology, thereby emphasizing the need to understand the molecular pathways that target these proteins to cilia (Cai et al., 2014).

Caenorhabditis elegans is a nematode worm that provides an excellent model for studying evolutionarily conserved ciliary processes, including those involved in the etiology of ADPKD. Adult hermaphrodite animals contain 302 neurons, including 60 ciliated sensory neurons (CSNs) that primarily reside in the head and tail of animals and that facilitate a variety of sensory modalities, including taste, smell, and touch. Male worms contain an additional 48 CSNs that are primarily involved in mating behaviors (Peden and Barr, 2005; Sulston, Albertson, & Thomson, 1980). The worm homologs of *PKD1 (lov-1)* and *PKD2 (pkd-2)* are expressed exclusively in male-specific CSNs and encode the protein products LOV-1 and PKD-2 respectively. LOV-1 and PKD-2 localize to and are shed from the tips of male-specific CSNs and are involved in regulating male-mating behaviors (Barr and Sternberg, 1999; Barr et al., 2001; O'Hagan, Wang, & Barr, 2014; Wang et al., 2014; Wang et al., 2015).

A number of previous pioneering studies applied proteomic comparisons of broad groups of taxa to identify core sets of evolutionary conserved ciliary components (Avidor-Reiss et al., 2004; Li et al., 2004). As the quality of genome sequencing data, including the curation of protein coding regions, has improved in the thirteen years since these studies, we hypothesized that additional analyses may emphasize the need to study some newly identified components over others. Our recent comparisons of algal and worm proteomes identified one such protein, the product encoded by the C05D10.2 locus in *C. elegans* (Henriksson, Piasecki, Lend, Burglin, & Swoboda, 2013). In addition to worms, the gene encoding this protein is present in humans, mice, fish, and the unicellular alga *Chlamydomonas reinhardtii* but not in organisms without cilia, including the yeast, *Saccharomyces cerevisiae*, or flowering plant, *Arabidopsis thaliana*. The protein product encoded at the *C. elegans* C05D10.2 locus is a putative ortholog of human mitogen activated kinase-15 (MAPK-15/ERK8). Pazour, Agrin, Leszyk, & Witman, (2005) first identified the MAPK-15 ortholog as a ciliary component in a proteomic analysis of isolated *C. reinhardtii* cilia. However, most mammalian studies of this protein have used nonciliated cell-culture lines to study the function of this protein (Chia, Tham, Gill, Bard-Chapeau, & Bard, 2014; Colecchia et al., 2012; Rossi et al., 2016).

Miyatake, Kusakabe, Takahashi, & Nishida (2015) recently showed that the *Xenopus* MAPK-15 ortholog ERK7 is involved in basal body positioning through interactions with the actin regulator CapZIP in multiciliated cells. However, MAPK-15 orthologs are found in ciliated organisms with reduced basal body structure, that lack CapZIP orthologs, and that do not contain multiciliated cells, including animals like nematode worms. Thus, it remains likely that MAPK-15 functions in additional evolutionarily conserved ciliary processes not previously described.

In this study, we show the MAPK-15 ortholog in *C. elegans* (MAPK-15) functions in cilia. Mutations in the *mapk-15* gene result in tail defects for both hermaphrodite and male animals, including defects in dye uptake and mating behavior respectively. Expression of *mapk-15* occurs exclusively in head and tail CSNs of both hermaphrodite and male worms, where its protein product localizes to cell bodies, dendritic processes, and cilia. Animals containing defects in *mapk-15* demonstrate aberrant PKD-2 protein localization.

2 | RESULTS

2.1 | *gk1234* Mutants have ciliary defects

Expressed-sequence tag data available on WormBase (www.wormbase.org), indicates that the C05D10.2 locus in *C. elegans* encodes three protein isoforms each containing between three and ten exons, including two isoforms (A and C) with a predicted kinase domain (Figure 1a; Harris et al., 2010). An allele containing a 1407bp deletion (*gk1234*) that removes all of exons five through seven and part of exon eight was generated as part of the *C. elegans* Deletion Mutant Consortium and obtained from the *C. elegans* Genetics Center (*C. elegans* Deletion Mutant Consortium, 2012). Bioinformatic analysis indicates that this allele contains a deletion in an aspartic acid residue (position number 137 in the amino acid sequence) that is required for the activity of the kinase domain for the A and C isoforms, but does not disrupt the small B isoform lacking this domain (Figure 1a; Jones et al., 2014). PCR amplification of genomic DNA followed by DNA sequencing confirmed the presence of the *gk1234* allele in VC2695 mutant worms, which were subsequently backcrossed to wild-type N2 worms for six generations to generate a near isogenic line.

To determine if animals homozygous for the *gk1234* allele contain any gross morphological ciliary defects, assays that exploit the ability of wild-type worms to take up a lipophilic dye were conducted. In comparison to wild-type worms that take up dye (DiI) in a subset of head (ADF, ADL, ASH, ASI, ASJ, ASK) and tail (PHA, PHB) CSNs, worms containing gross ciliary defects, including the complete absence of cilia in *che-13*(*e1805*) mutant worms, show a complete dye-filling defective or Dyf phenotype (Figure 1b). Interestingly, worms homozygous for the *gk1234* allele have a Dyf phenotype that exclusively affects tail CSNs (PHA and PHB), a phenotype that is ~95% penetrant (Figure 1b).

A closer analysis of C05D10.2(*gk1234*) mutant animals found no discernable defects in dye uptake in head CSNs but did find additional defects in the few (~5%) tail CSNs that were able to uptake dye. Quantification of dye-uptake revealed staining in dorsal (ADL, ASI, ASK) and ventral (ADF, ASH, and ASJ) amphid neurons on the left and right side for both C05D10.2(*gk1234*) mutants that was statistically indistinguishable from wild-type animals (Figure 2a–c). In comparison only 19% of C05D10.2(*gk1234)* mutant animals with phasmid dye uptake had staining on both sides, as is always observed in wild-type

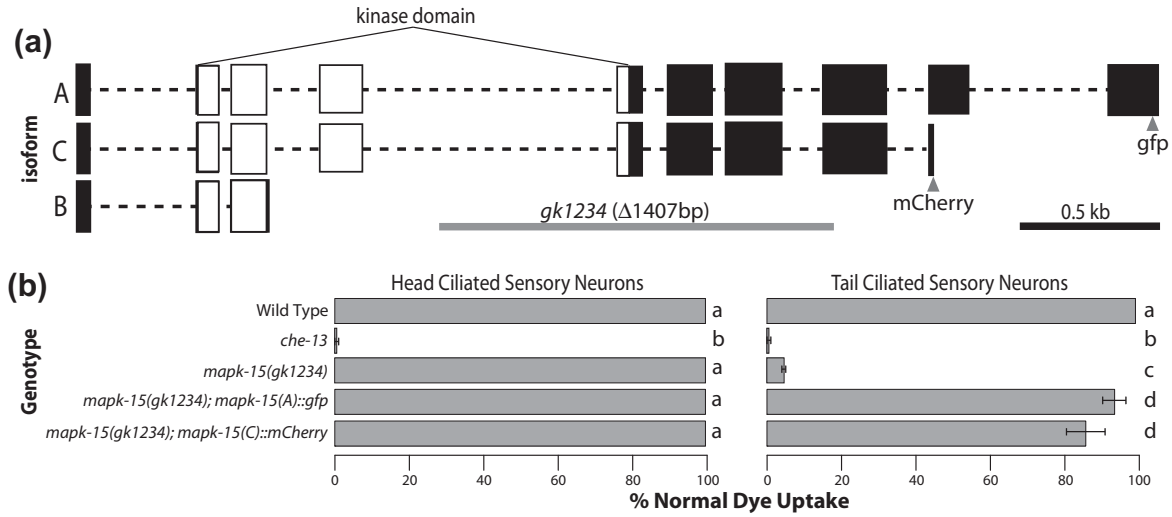

FIGURE 1 MAPK-15 is required for efficient dye uptake in tail CSNs. (a) The *mapk-15* locus encodes three distinct isoforms, two of which contain a full-length kinase domain (white boxes). The *gk1234* allele (gray line) is missing exons (white and black boxes) 5–7 and part of 8 for both isoforms A and C. Genetic constructs containing carboxy-terminal fluorescent tags were generated for A and C isoforms (arrow heads). (b) Animals containing the *mapk-15(gk1234)* deletion contain a robust tail-specific dye-filling defect, which can be rescued with genomic constructs expressing fusion proteins for either isoforms A or C. Values represent four trial averages for the proportion of worms that dye fill in head and tail CSNs for each of the respective genotypes where n >50 worms/trial. Error bars represent standard deviation. Mann-Whitney U tests were used to do comparative statistics; genotypes that are significantly different from each other ($p < .05$) are labeled with different letters

animals (Figure 2d–f). The remaining 81% of worms stained randomly on one side or the other. Interestingly, phasmid neurons (PHA and PHB) stained in pairs (left or right) 96% of the time. Thus, the *gk1234* allele confers a subtle but robust Dyf phenotype that exclusively affects phasmid tail neurons. Contrary to the observed phenotype of *ccpp-1* mutant animals, a mutation that also confers a subtle Dyf phenotype (O'Hagan et al., 2011), no osmosensory defects to glycerol were observed in a *gk1234* homozygous strain (Figure 2g).

Tail specific dye-filling defective phenotypes were previously linked to dendritic extension defects caused by mutations in genes affecting the transition-zone region at the base of cilia (Schouteden, Serwas, Palfy, & Dammermann, 2015; Williams, Winkelbauer, Schafer, Michaud, & Yoder, 2008; Williams et al., 2011). To differentiate between ciliary assembly and dendritic extension defects the transition zone component NPHP-1 fused to cyan fluorecent protein (CFP) was examined in the dye-filled phasmid neurons of wild-type and C05D10.2(*gk1234*) mutant animals. Fluorescent NPHP-1 foci in wild-type worms were observed at positions approximately equidistant from the most posterior end of the tail on left and right sides of animals (Figure 2h). Whereas, NPHP-1 foci were consistently observed to be more anterior in dye-filling defective neurons than in neurons able to take up dye, suggesting that there may be dendritic extension defects in C05D10.2(*gk1234*) mutant animals (Figure 2h).

Analysis of a *mapk-15* promoter to *mCherry* fusion construct in C05D10.2(*gk1234*) mutant animals confirmed dendritic extension defects in phasmid CSNs. In wild-type worms, dendrites are approximately equal length and contain NPHP-1 foci at their dendritic tips (Figure 3a). In comparison, dendritic processes in C05D10.2(*gk1234*) mutant animals appear disorganized and of variable lengths (Figure 3b–d). Dendritic processes were sometimes observed to be shortened with NPHP-1 foci at their distal tips (Figure 3b,c). While, occasionally NPHP-1 foci were observed at the base of or somewhere along the length of disorganized but extended dendritic projections (Figure 3d). As compared to wild-type worms, dendritic lengths were significantly shorter and of more variable lengths in C05D10.2(*gk1234*) mutant animals (Figure 3e).

2.2 | MAPK-15 rescues the *gk1234* mutant phenotype

Gene-to-fluorescent protein fusion constructs under control of their native promoters for either the A and C isoforms encoded at the C05D10.2 locus were able to rescue the Dyf phenotype of worms homozygous for the *gk1234* allele when expressed as individual transgene arrays (Figure 1a,b). Rescue of strains expressing the A- or C-isoform were ~95 and 86% penetrant, respectively, but were statistically indistinguishable from each other. No aberrant dendrites were observed in either rescue strain. It should be noted that the full-length genomic construct for the A isoform should express the intermediate length C product, without its corresponding fluorescent tag. Thus, these data demonstrate that the C-isoform is sufficient to rescue the Dyf phenotype of the *gk1234* allele and that presence of the fused fluorophores for either isoform A or C do not disrupt the ciliary function of these gene products. We hereby refer to the gene encoded by the *C. elegans* C05D10.2 locus as *mapk-15*.

2.3 | *mapk-15*/MAPK-15 is expressed in, and localizes to, CSNs

Analysis of individual strains expressing either fluorescent-tagged *mapk-15* A- or C-specific isoforms in hermaphrodite animals

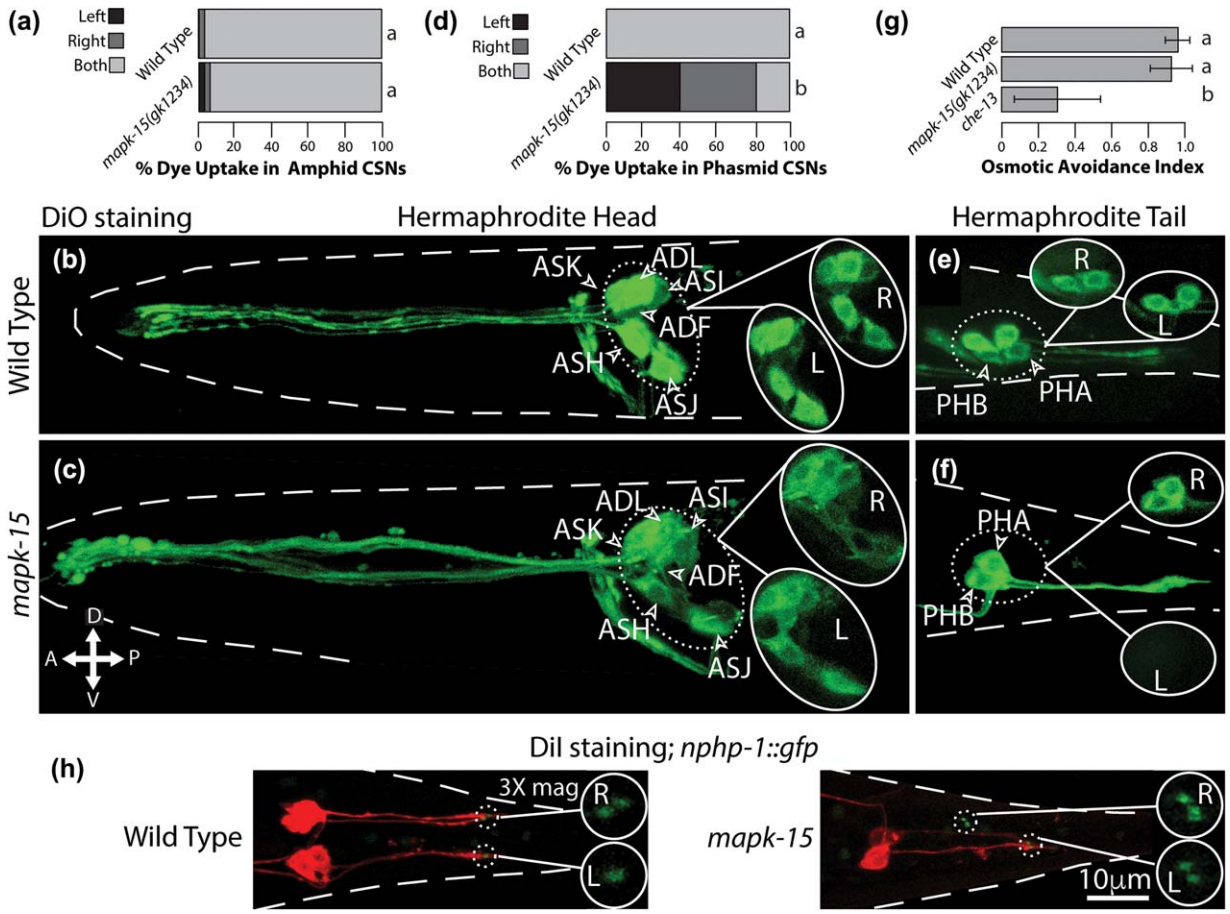

FIGURE 2 Quantification and characterization of the Dyf phenotype in *mapk-15(gk1234)* mutant worms. (a) Quantification of dye uptake in amphid CSNs on the right and/or left side of wild-type and *mapk-15(gk1234)* mutant worms. Values represent the proportion of 30 animals showing dye uptake in all six amphid CSNs on either or both side(s) of the head. (b,c) Confocal projections through animal heads (dashed line) showing dye-uptake in amphid CSNs in wild-type and *mapk-15(gk1234)* mutant worms. Cutouts show the subset of focal planes containing only left (L) or right (R) sides of worms. The respective orientation of each panel, including anterior (A), posterior (P), dorsal (D), and ventral (V) sides, is indicated in the key. (d) Quantification of dye uptake in phasmid CSNs on the right and/or left side of wild-type and *mapk-15(gk1234)* mutant worms. Values represent the proportion of 50 animals showing dye uptake on either or both side(s) of the tail. (e,f) Confocal projections through tail region of worms (dashed line) showing dye-uptake in phasmid CSNs in wild-type and *mapk-15(gk1234)* mutant animals. Cutouts show the subset of focal planes containing only left or right sides of worms. (g) Quantification of the osmotic avoidance index of wild-type, *mapk-15(gk1234)*, and *che-13(e1805)* mutant worms. Values represent the average osmotic avoidance index of eight to eleven trials, with 6 worms/trial. Error bars represent standard deviation. Mann-Whitney U tests were used to do comparative statistics; genotypes that are significantly different from each other ($p < .05$) are labeled with different letters. (h) Confocal projections of wild-type or *mapk-15(gk1234)* mutant worms expressing *nphp-1* fused to *cfp* (green), stained with DiI (red). Cutouts show three times enlarged NPHP-1 foci [Color figure can be viewed at wileyonlinelibrary.com]

demonstrated robust expression of both products exclusively in CSNs (Figure 4a–d). Expression of isoform A-fused to *gfp* and C-fused to *mCherry* was observed in non-dye-filling (ASE, BAG, CEP, IL1, IL2, and OLQ) and dye-filling (ADL, ADF, ASH, ASI, ASJ, and ASK) head CSNs, as well as in nondye filling (PQR) and dye filling (PHA, PHB) tail CSNs. Expression was also occasionally observed in mid-body neurons (PDE). Thus, *mapk-15* is more broadly expressed than would be predicted based on the tail-specific Dyf phenotype of mutant *mapk-15*(*gk1234*) worms.

MAPK-15 isoforms A and C show similar localization patterns. Isoform A localizes broadly to cell bodies, dendritic processes, and throughout the ciliary region of CSNs (Figure 4a,b). Isoform C primarily localizes to cell bodies in punctate spots and throughout the ciliary region of CSNs, with only a diffuse signal along dendritic processes (Figure 4c,d). Within the ciliary region, localization of both A and C isoforms occurs in a region consistent with the periciliary membrane compartment (PCMC) and along the length of the cilium. Analysis of a strain expressing the fluorescently tagged PCMC marker *kap-1* demonstrated MAPK-15 isoform C colocalization with KAP-1 in the PCMC (Figure 4e). Analysis of a strain expressing the fluorescently tagged transition-zone marker *nphp-1* demonstrated that MAPK-15 isoform C does not colocalize with NPHP-1 in the transition zone, which resides between the PCMC and cilium (Figure 4f).

A cross between strains expressing the *gfp*-tagged A isoform and *mCherry*-tagged C isoform generated a strain expressing both fusion proteins. Analyses of double-transgenic worms were consistent with

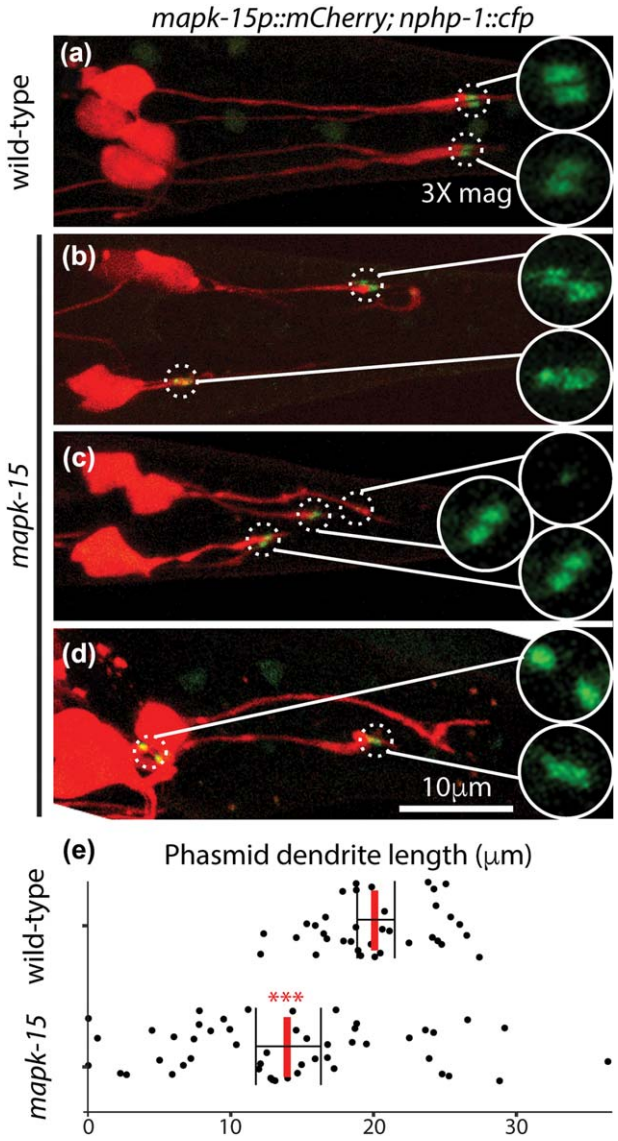

FIGURE 3 Characterization and quantification of *mapk-15 (gk1234)* dendritic extension defects. Confocal projections of (a) wild-type and (b–d) *mapk-15(gk1234)* mutant worms expressing the *mapk-15* promoter fused to *mCherry* (red) and *nphp-1* fused to *cfp* (green). (e) Quantification of phasmid dendrite length, measured from the posterior cell body to the NPHP-1 foci in confocal projections. Solid red lines represent the mean. Error bars represent standard deviation. A two-sample, unpaired t test revealed that dendritic length is significantly different in *mapk-15(gk1234)* animals as compared with wild-type animals ($p < .0001$), indicated by *** on the plot [Color figure can be viewed at wileyonlinelibrary.com]

strains harboring individual transgenes (Supporting Information Figure S1A-F). However, an increased expression of isoforms A and C was observed in dopaminergic neurons (CEP and ADE) and a reduction in the intensity of the ciliary-localized C isoform were observed, results that were not replicated in a strain expressing endogenous wild-type *mapk-15* together with the transgenic-isoform C array (Supporting Information Figure S1G-J). Thus, MAPK-15 isoforms A and C both localize to the cell body, dendritic process, and ciliary regions of a large set of head and tail CSNs.

2.4 | *mapk-15*/MAPK-15 is expressed in and localizes to male CSNs

Males containing either the fluorescent-tagged A- or C-protein isoforms showed expression in tail HOB and all 9 Rn CSNs (Figure 5a,b). Localization of the A- and C-protein isoform products was found in the cell body, dendritic projections, and ciliary regions, similar to the localization pattern observed in hermaphrodite animals, with ciliary staining more discernable from dendritic process staining in the C-isoform. Consistent with our observation in hermaphrodites, double-transgenic male animals also demonstrated increased expression of isoforms A and C in the male dopaminergic neurons (Rn 5, 7, and 9) and a reduction in the intensity of the ciliary-localized C isoform (Supporting Information Figure S2A-C). However, these results were again not replicated in a strain expressing endogenous wild-type *mapk-15* together with the transgenic-isoform C array (Supporting Information Figure 2D). Analysis of a strain expressing the *nphp-1* and *mapk-15* isoform C constructs demonstrated localization primarily to a single neuron of each Rn A/B pair. However, neurons 2, 3, and 6 consistently appear to show expression of both *nphp-1* and *mapk-15* constructs in both Rn A and B neurons, with one typically containing higher expression than the other (Figure 5c). Analysis of a *mapk-15* promoter-to-*mCherry* fusion construct demonstrated expression in head CEM CSNs, as indicated by a *pkd-2* gene-to-*gfp* marker (Supporting Information Figure 3A-C). Interestingly, the *mapk-15* promoter-to-*mCherry* fusion construct in *mapk-15(gk1234)* mutant animals demonstrated no aberrant dendritic processes in male ray neurons as was previously observed in phasmid neurons (compare Figures 3 and 5d).

2.5 | MAPK-15 is required for male mating behavior

Because of the robust expression of *mapk-15* in male ray neurons, we wished to determine if MAPK-15 affects male mating behavior. The mating efficiency of *mapk-15(gk1234)* mutant worms was compared to that of normal mating *him-5(e1490)* worms. Mutant and normal-mating males were each separately crossed with homozygous *dpy-17(e164)* hermaphrodites, which confers a recessive dumpy (Dpy) phenotype that is readily distinguishable from non-Dpy worms. Therefore, only outcrossed progeny of Dpy hermaphrodites will be non-Dpy via heterozygosity. As compared to normal-mating worms, *mapk-15(gk1234)* mutant worms have a pronounced male-mating defect that results in a complete lack of male mating under the conditions of this assay, results that are statistically indistinguishable from a strain harboring a *daf-19 (m86)* mutation that results in a complete absence of cilia (Figure 5e). Similar to the results of the *mapk-15(gk1234)* dye-filling rescue experiments, the presence of either the A or C isoforms are able to rescue the male mating defects in mutant worms to a level indistinguishable from wild-type animals.

The male mating pathway in worms is comprised of several distinct behaviors, including hermaphrodite location, vulva localization, spicule injection, and copulation (Barr and Garcia, 2006; O'Hagan et al., 2014). Preliminary observations indicated that *mapk-15(gk1234)* mutant worms were defective at early stages of the mating process. To

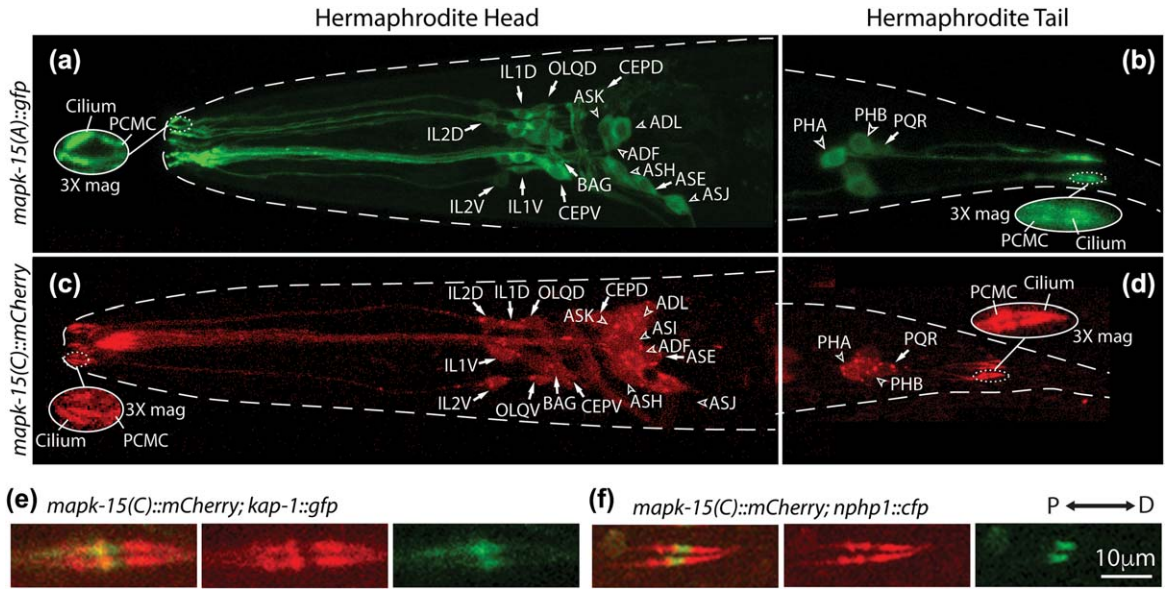

FIGURE 4 **Expression and localization of *mapk-15*/MAPK-15 occurs in head and tail CSNs of hermaphrodite animals.** Confocal projections of *mapk-15(gk1234)* mutant worms expressing *mapk-15* (a,b) isoform A fused to *gfp* (green) and (c,d) isoform C fused to *mCherry* (red). Expression in non-dye filled (solid arrows) and dye-filled (open arrow heads) CSNs are indicated. Cutouts show three times enlarged ciliary regions for head and tail CSNs. Head and tail regions of worm bodies are indicated (dashed lines). Confocal projections of wild-type worms expressing *mapk-15* isoform C fused to *mCherry* (red) with (e) *kap-1* fused to *gfp* (green) or (f) *nphp-1* fused to *cfp* (green) in a single pair of phasmid cilia enlarged three times. The respective orientation of each panel, including proximal (P) and distal (D) ends, is indicated in the key [Color figure can be viewed at wileyonlinelibrary.com]

examine this observation, an assay that determines the response rate of a male upon contact with an uncoordinated *unc-31(e169)* hermaphrodite, which is less likely to move away from a male, was conducted (Barr and Sternberg, 1999). As compared with normal mating *him-5 (e1490)* worms, animals homozygous for *mapk-15(gk1234)* contain robust and statistically significant hermaphrodite response defects (Figure 5f). However, the observed defect in *mapk-15(gk1234)* mutant worms is not as pronounced as that of the strain harboring a *daf-19 (m86)* mutation. Thus, *mapk-15(gk1234)* mutant males are defective at an early step of the male-mating pathway.

2.6 | Polycystin 2 is mislocalized in *mapk-15(gk1234)*

Peden and Barr (2005) demonstrated that PKD-2 is mislocalized in a number of male mating mutants whose protein products have similar expression and localization patterns to MAPK-15. The mislocalization of PKD-2 to cilia is known as a ciliary-localization defective or Cil phenotype. A strain expressing a *pkd-2* gene-to-*gfp* fusion construct was crossed into *mapk-15*(*gk1234*) mutant animals and the localization of its gene product was compared to its normal-mating parent. As previously demonstrated, PKD-2 localizes to the tips of *him-5(e1490)* normal-mating worms (Figure 6a,b). In comparison *mapk-15(gk1234)* mutant worms contain a Cil phenotype, which results in PKD-2 localization occurring more broadly to the dendrites, ciliary base, and ciliary shaft (Figure 6c,d; Peden and Barr, 2005). Thus, MAPK-15 function is likely upstream of PKD-2 localization.

2.7 | Expression of *mapk-15* with the *pkd-2* promoter rescues male mating defects

The mating defect observed for *mapk-15(gk1234)* mutant animals appeared more pronounced than those previously reported for a strain harboring the null allele *pkd-2(sy606)*. Therefore, the mating efficiency of *pkd-2(sy606)* and *mapk-15(gk1234)* mutant strains, as well as a strain expressing the *mapk-15* gene under control of the *pkd-2* promoter were compared. As expected, worms containing a *pkd-2(sy606)* mutation were statistically distinguishable from wild-type worms but contained a less severe response defect than *mapk-15(gk1234)* mutant animals (Figure 6e). Interestingly, a strain expressing a the full-length *mapk-15* gene under control of the *pkd-2* promoter was able to largely rescue the male mating response defect observed in the *mapk-15 (gk1234)* mutant strain, but rescue of this strain was not as high and remained statistically distinguishable from the wild-type strain and a *mapk-15(gk1234)* mutant strain rescued with the *mapk-15* gene under the control of its native promoter (Figure 6e). Thus, a strain expressing *mapk-15* exclusively in *pkd-2* expressing cells is able to partially rescue the male response defect conferred by the *mapk-15(gk1234)* mutation.

2.8 | Expression of *mapk-15* is dependent on DAF-19 in some cells

In animals, many ciliary genes contain x-box promoter motifs in their respective upstream *cis* regulatory regions (Piasecki, Burghoorn, & Swoboda, 2010). These ~13–15bp motifs are bound and positively regulated by regulatory factor X (RFX) transcription factors (Burghoorn

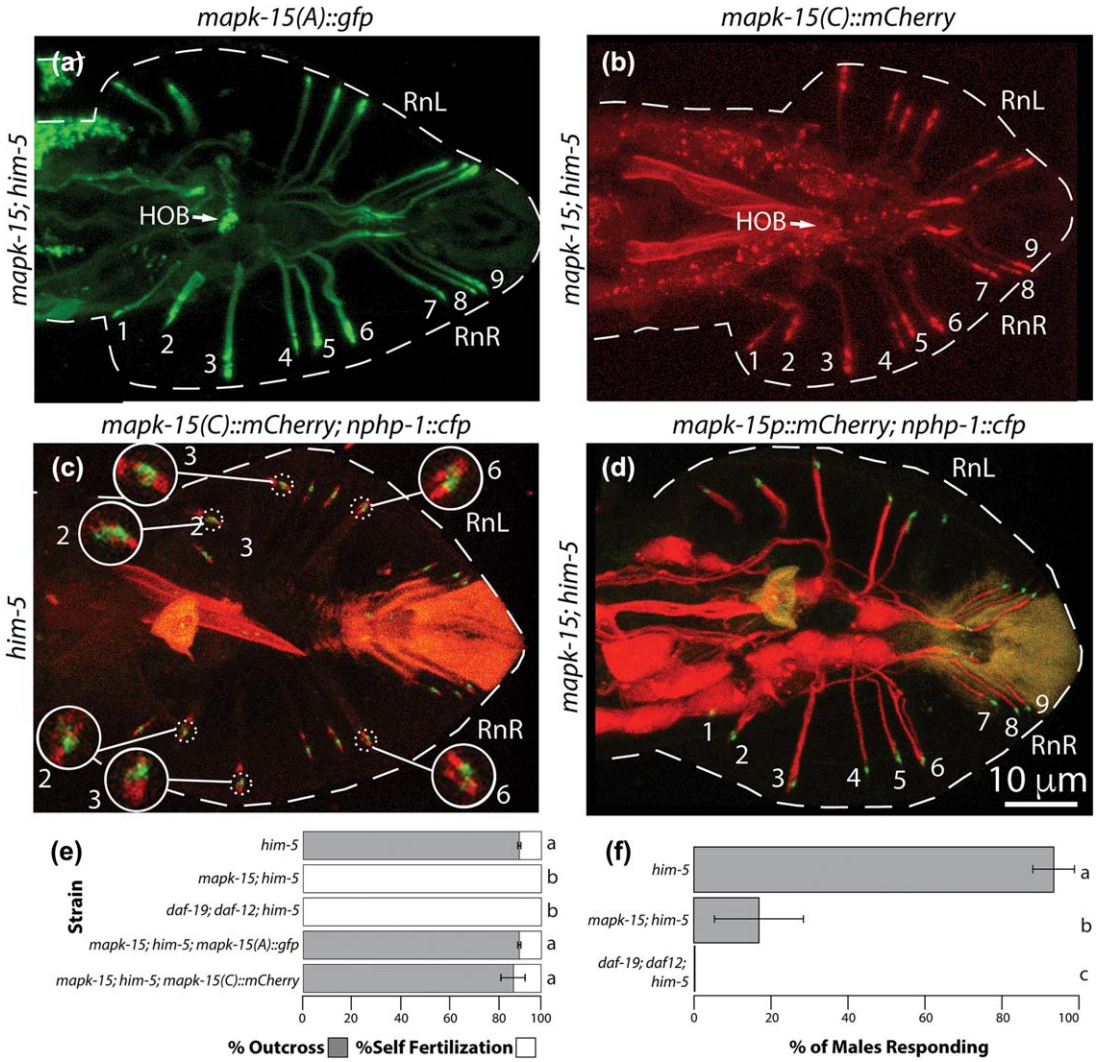

FIGURE 5 Expression and localization of *mapk-15*/MAPK-15 occurs in male tail CSNs, and *mapk-15(gk1234)* mutant worms harbor male mating defects. Confocal projections of *mapk-15(gk1234)* mutant worms expressing *mapk-15* (a) isoform A fused to *gfp* (green) and (b) isoform C fused to *mCherry* (red). (c) Confocal projection of *mapk-15(gk1234)* mutant worms expressing *mapk-15* isoform C fused to *mCherry* (red) and *nphp-1* fused to *cfp* (green). (d) Confocal projection of *mapk-15(gk1234)* mutant worms expressing the *mapk-15* promoter fused to *mCherry* (red) and *nphp-1* fused to *cfp* (green). Numbers indicate the specific ray neuronal projection. Tail regions of worm bodies are indicated (dashed lines). (e) Mutant *mapk-15(gk1234)* worms harbor male mating defects, which can be rescued with either the A- or C-isoform transgene. Values represent average proportions of outcrossed as compared to self-fertilized progeny of four individual mating experiments for each strain. Mann-Whitney U tests were used to do comparative statistics. (f) Mutant *mapk-15(gk1234)* worms harbor a hermaphrodite response defect. Values represent the proportion of male worms of each strain responding to a hermaphrodite within 10 min with 60 worms/strain. Error bars represent standard deviation. A generalized linear model using a binomial distribution was used to do comparative statistics; genotypes that are significantly different from each other ($p < .05$) are labeled with different letters [Color figure can be viewed at wileyonlinelibrary.com]

et al., 2012). Blacque et al., (2005) identified a putative x-box promoter motif 214bp upstream of the *mapk-15* coding region. However, this sequence resides further upstream than most CSN-specific genes with broad expression patterns, which typically contain x-box promoter motifs 100bp or less upstream of the transcriptional start site (Burghoorn et al., 2012).

To determine if *C. elegans mapk-15* contains a functional x-box promoter motif, expression of a *mapk-15* promoter-to-*mCherry* transcriptional fusion construct was compared in the presence and absence of *daf-19*, the sole RFX-type transcription factor in *C. elegans* (Figure 7a–h). A transcriptional fusion construct was selected for these comparisons over a translational construct because *daf-19(m86)* mutant worms lack cilia and fluorescent-tagged ciliary proteins may be less stable in this background, thus making it difficult to tease apart expression from stability and/or localization differences. As previously observed for the A- and C-isoform translational fusion constructs, young adults containing a wild-type copy of the *daf-19* gene demonstrate robust expression of the *mapk-15* transcriptional-fusion construct in head and tail CSNs of both hermaphrodite and male animals. However, expression of the *mapk-15* transcriptional construct was additionally found in the head neurons AFD, ADE, and ASG, as distinguished from other neurons based on their proximity to known dye-filled neurons (Figure 7a,b).

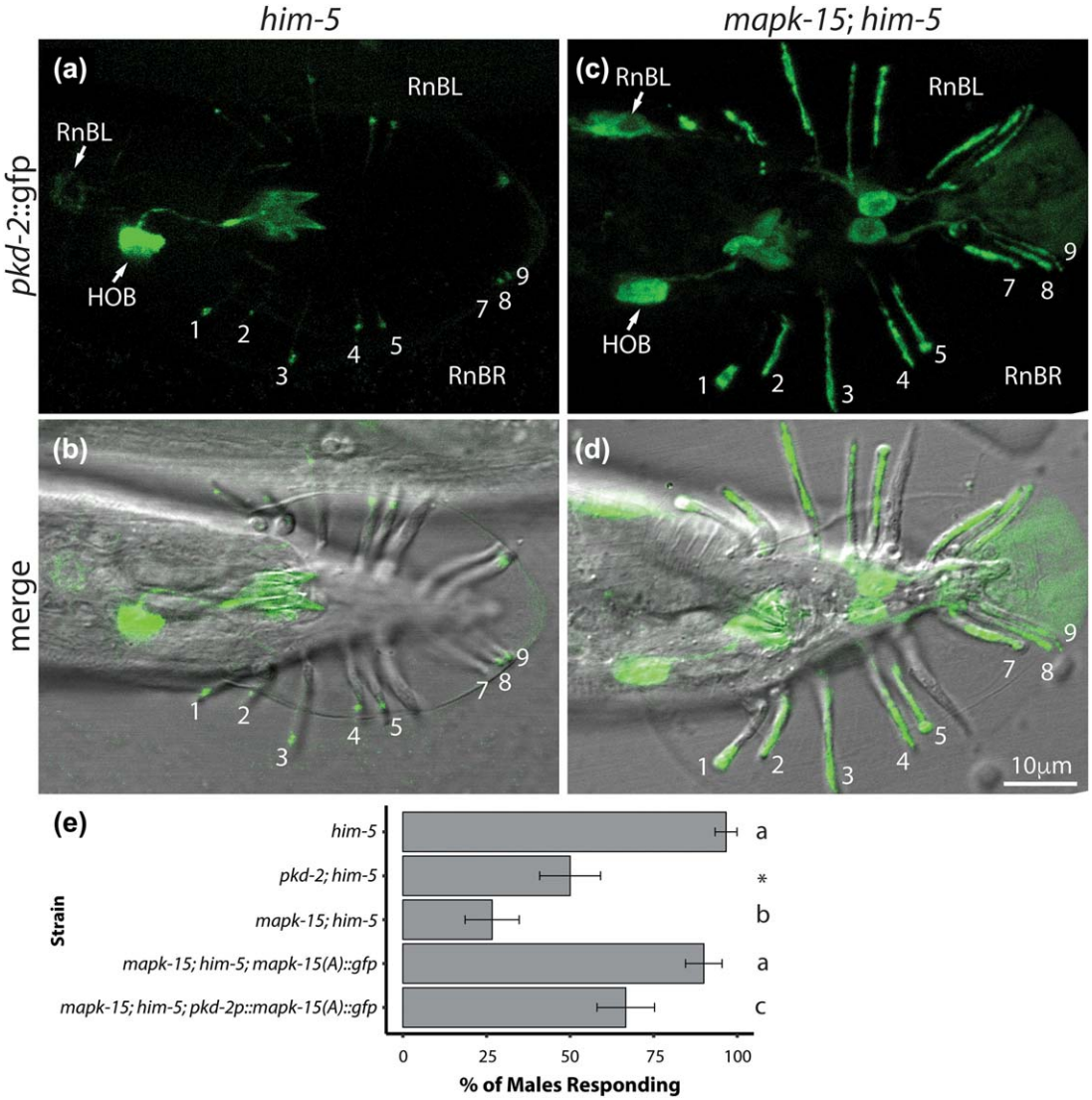

FIGURE 6 **PKD-2 is mislocalized in *mapk-15(gk1234)* mutant animals.** PKD-2 fused to GFP (a,b) localizes to ciliary tips of normal mating *him-5 (e1490)* males and (c,d) along the dendritic processes and the entire ciliary region in *mapk-15(gk1234)* mutant worms. (a,c) Fluorescent images alone or (b,d) in combination with their respective DIC image are shown. Expression in neuronal cell bodies (solid arrows) are depicted, numbers indicate the specific ray neuronal projection next to its associated ciliary region. (e) The hermaphrodite response defect harbored by male *mapk-15(gk1234)* worms is rescued by the *mapk-15* transgene driven by either the native or *pkd-2* promoter. Values represent the proportion of male worms of each strain responding to a hermaphrodite within 10 min with 30 worms/strain. Error bars represent standard deviation. A generalized linear model using a binomial distribution was used to do comparative statistics; genotypes that are significantly different from each other ($p < .05$) are labeled with different letters; asterisk is different from group A only [Color figure can be viewed at wileyonlinelibrary.com]

In comparison, the *mapk-15* transcriptional fusion construct was differentially expressed in *daf-19(m86)* mutant animals. Mutant worms retained robust expression of *mapk-15* in amphid dorsal and ventral head neurons of young adult animals, similar to that observed in wild-type worms (Figure 7a–c). Interestingly, expression of *mapk-15* was not observed in IL2 neurons of *daf-19(m86)* mutant worms but was considerably more intense in IL1 neurons. IL1 and IL2 neurons were distinguished from each other based on their respective shape and relative position to the nerve ring. Expression of *mapk-15* in the hermaphrodite phasmid neurons PHA and PHB was absent in the *daf-19(m86)* mutant worms, while expression remains robust in PQR. As seen in *him-5(e1490)* males, *mapk-15* is expressed in HOB and all Rn CSNs (Figure 7g,h), whereas, expression was consistently diminished in HOB and Rn CSNs in *daf-19(m86)* mutant animals. Thus, *mapk-15* expression appears to be RFX-dependent in IL2, PHA, PHB, HOB, and Rn CSNs, down regulated by DAF-19 in IL1 CSNs, and RFX-independent in all other *C. elegans* head and tail CSNs.

3 | DISCUSSION

Here we report that *C. elegans mapk-15* is required for CSN function but is not required for ciliary formation. Transcriptional and translational fusion constructs demonstrated that *mapk-15* is expressed in

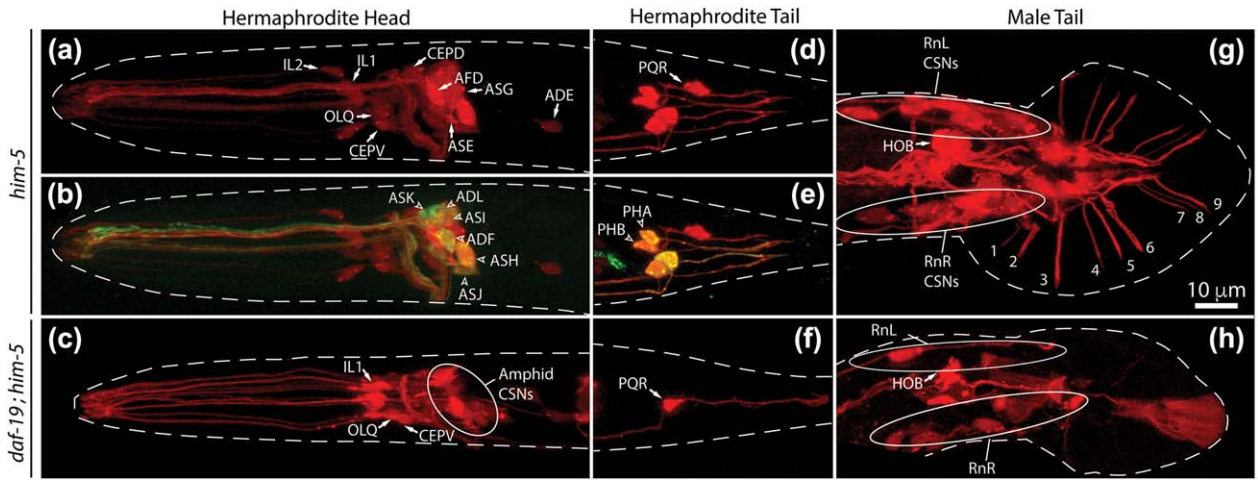

FIGURE 7 Expression of the *mapk-15* occurs in head and tail CSNs of hermaphrodite and male animals. Confocal projections of wild type or *mapk-15(gk1234)* mutant (a–c) hermaphrodite heads, (d–f) hermaphrodite tails, and (g,h) male tails for strains expressing the *mapk-15* promoter fused to *mCherry* (red) alone or (b, e) in combination with DiO stained neurons (green). CSNs that typically do not dye fill (solid arrows) and those that typically do (open arrow heads) are indicated. Circled regions represent areas with robust expression. (g,h) Numbers indicate the specific male ray neuronal projection next to its associated ciliary region. Head and tail regions of the worm bodies are indicated (dashed lines) [Color figure can be viewed at wileyonlinelibrary.com]

many head and tail CSNs of both hermaphrodite and male worms, including CSNs that are capable of taking up lipophilic dyes (Figure 4a–d; Supporting Information Figure S1A-J). The ability of specific CSNs to uptake dye suggests that the overall morphological integrity of cilia is present in these cells (Perkins, Hedgecock, Thomson, & Culotti, 1986; Starich et al., 1995). Importantly, dye uptake in amphid CSNs of *mapk-15(gk1234)* mutant worms was statistically indistinguishable from wild-type worms (Figures 1b and 2a). Thus, the uptake of dye in amphid CSNs indicates that amphid cilia are relatively structurally complete in *mapk-15(gk1234)* mutant animals. Consistent with these results, PKD-2 localization was observed throughout what appears to be intact ciliary regions in the male tail of *mapk-15(gk1234)* mutant worms (Figure 6c,d), despite the observation that this strain harbors male-mating defects that have been attributed to ciliary functions of these CSNs (Figure 5e,f; Barr and Sternburg, 1999).

In comparison to the normal dye filling observed in head CSNs, dye uptake was aberrant in the tail of most but not all hermaphrodite *mapk-15(gk1234)* mutant worms (Figures 1b and 2d–f), a result which more likely reflects an inability of animals to fully extend their dendritic processes than a structural defect of cilia. Support for this is provided by several observations. First, some (<5%) phasmid CSNs are able to dye fill normally and the fluorescent product of the transcriptional *mapk-15* fusion construct extends distally past NPHP-1 foci (Figures 2d and 3a–d), indicating the presence of phasmid cilia despite phasmid dye-filling defects. Second, the few animals that are able to take up dye in one set of left or right PHA and PHB neuronal pairs contained NPHP-1 foci that were always positioned more posterior to NPHP-1 foci residing in the dye-filling defective PHA and PHB neuronal pair (Figure 2h), suggesting that the longer dendritic projections are more likely to function properly. Finally, wild-type worms contained longer (on average), less variable, and more highly organized dendritic processes than *mapk-15(gk1234)* mutant worms (Figure 3a–e). Interestingly, the dendritic processes of male ray neurons appear to be fully intact in *mapk-15(gk1234)* mutant animals, despite an inability of this strain to mate efficiently (Figure 5d–f). Taken together, these data suggest that *mapk-15* is not essential for ciliogenesis in *C. elegans* but that *mapk-15* likely functions in sensory-specific pathways like mate finding.

The dendritic processes of most CSNs develop through a process called retrograde extension, which involves dendritic formation occurring simultaneously to the cell body pulling away from the ciliary base that is firmly anchored in place during embryonic development (Sulston, Albertson, & Thomson, 1980). Several previous reports have linked a variety of transition-zone components to the anchoring ability of the ciliary base, including complexes containing several Meckel-Gruber syndrome and NPHP protein components (Schouteden et al., 2015; Williams et al., 2008, 2011). Interestingly, *mapk-15* also appears to affect the adhesion of the ciliary base. However, to our knowledge this is the first PCMC component linked to the fidelity of retrograde extension.

ERK7 is the *Xenopus* ortholog of *C. elegans* MAPK-15, which was recently linked to ciliary assembly defects during *Xenopus* development (Miyatake et al., 2015). Basal body migration defects were observed in *erk7* deficient cells, likely involving interactions with actin at the cell surface. It will be interesting to explore the possibility that the docking of basal bodies to the surface of *Xenopus* cells and the anchoring of cilia at dendritic tips involves similar molecular pathways.

Several lines of evidence suggest that the MAPK-15 protein functions upstream of PKD-2 to modulate the ability of males to locate hermaphrodites. First, mutations in *pkd-2(sy606)* and *mapk-15(gk1234)* both result in early stage male-mating defects, while the former has subtler and the latter more pronounced defects (Figure 6e). Second, the PKD-2 protein is mislocalized in *mapk-15(gk1234)* mutant animals (Figure 6c,d). Third, expression of the *mapk-15* gene by the *pkd-2* promoter was able to largely, but not entirely rescue the mating defects of

mapk-15(gk1234) mutant worms, despite *mapk-15* being much more broadly expressed in wild-type worms (Figures 5a–d and 6a,e). Collectively, these data suggest that *mapk-15* functions upstream of *pkd-2* in RnB-type neurons to modulate the ability of males to locate hermaphrodites. However, our observation that *mapk-15* is also expressed in at least three RnA-type neurons and the two RnB neurons that do not express *pkd-2* raises the possibility that these neurons may also contribute to additional mating functions (Figure 5c).

Localization of PKD-2 in *mapk-15(gk1234)* mutant animals appears to phenocopy that of *klp-6(sy511)*, *ccpp-1(ok1821)*, and *cil-7(my16)* mutant animals, which are also male-mating defective mutants with Cil phenotypes that exhibit less severe or nonexistent dye-filling defects (Maguire et al., 2015; O'Hagan et al., 2011; Peden and Barr, 2005). Similar to *klp-6(sy511)*, *ccpp-1(ok1821)*, and *cil-7(my16)* mutant animals, *mapk-15(gk1234)* mutant animals show more pronounced PKD-2 localization along the entire length of the cilium and dendritic processes than is observed in normal mating worms (Figure 6a–d). KLP-6 is a kinesin-3 protein required for EV release (Peden and Barr, 2005; Wang et al., 2014), CCPP-1 is a tubulin deglutamylase that maintains axonemal stability (Kimura et al., 2010; O'Hagan et al., 2011), and CIL-7 is a myristoylated protein that likely functions in targeting proteins for vesicular trafficking (Maguire et al., 2015). As such, *mapk-15* may also function in a vesicular transport or cytoskeletal modifying process that is required for PKD-2 targeting to cilia.

The *daf-19* gene in *C. elegans* encodes for at least four specific isoforms that typically act as activators but occasionally as repressors of gene expression, (Chu et al., 2012; Swoboda, Adler, & Thomas, 2000; Wang, Schwartz, & Barr, 2010). Despite being exhaustively characterized in *C. elegans*, the same x-box motif has never been found to act as both an enhancer and repressor of ciliogenesis (Blacque et al., 2005; Efimenko et al., 2005; Chen et al., 2006; Burghoorn et al., 2012). Here, we find that CSN expression of *mapk-15* appears to be activated by DAF-19 in some CSNs (PHA, PHB, IL2, HOB, and Rn), while *mapk-15* may be down regulated by DAF-19 in other CSNs (IL1) (Figure 7a–h). Additionally, expression of *mapk-15* in many CSNs appears to be DAF-19 independent, indicating a novel mode of regulation in these CSNs (e.g. in all amphid and PQR CSNs).

4 | MATERIALS AND METHODS

4.1 | Generation of plasmid constructs for transgenesis

Promoter- and gene-fusion constructs were generated using PCR amplification, followed by restriction digestion, and ligation into an expression vector. N2 (wild-type) genomic DNA was used as a template for all constructs. PCR amplification of *mapk-15* isoform A used NEB Phusion ® High-Fidelity polymerase (New England Biolabs, Ipswich, MA, USA), while amplification of *mapk-15* isoform C, the *mapk-15* promoter, and the *pkd-2* promoter used Q5® High-Fidelity DNA Polymerase (New England Biolabs). Amplicons of *mapk-15* included a promoter region beginning between 856 and 1128bp upstream of its translational start site. Upon PCR amplification the *mapk-15* isoform A was A-tailed and ligated into the pGEM-T (Promega, Madison, WI) vector, prior to being digested and ligated into the Andrew Fire lab (Stanford School of Medicine, Stanford, CA) vector pPD95.77. The *mapk-15* isoform C PCR product was directly cloned into vector PSO522, which contains the pPD95.77 vector with *mCherry* substituted for *gfp*. The *mapk-15* promoter product was cloned directly into PSO576, which is the pPD95.75 vector with *mCherry* substituted for *gfp*. The *mapk-15* isoform A construct under control of the *pkd-2* promoter was generated by fusing the 934bp *pkd-2* promoter amplicon to a KpnI site found 18bp upstream of the translational start site for the full length *mapk-15* isoform A construct. Transcriptional and translational fusion constructs were introduced in the *C. elegans* germline by microinjection at 20–30 and 1–3 ng/μL, respectively (Mello and Fire, 1995).

4.2 | Strains and growth conditions

All strains were cultured at 20°C using standard procedures (Brenner, 1974). Bristol N2 was used as a wild-type strain. Strains CB164 *dpy-17 (e164) III*, CB169 *unc-31(e169) IV*, and PT9 *pkd-2(sy606) IV*; *him-5 (e1490) V* were used in male-mating behavior assays. CB3323 *che-13 (e1805) I* was used as a negative control in dye uptake and osmotic avoidance assays. CB4088 *him-5(e1490) V* was used as a normal mating control and in genetic crosses to generate strains with a high incidence of males. OE3492 *daf-19(m86) II*; *daf-12(sa204) X*; *him-5(e1490) V* and OE3738 *daf-12(sa204) X*; *him-5(e1490) V* were used in male mating assays and for examining the DAF-19/RFX dependence of the promoter-fusion construct. PT443 *pkd-2(sy606) IV*; *him-5(e1490) V*; myIs1[*pkd-2::gfp* + *unc-122p::gfp*] was used in PKD-2 localization and CEM identification studies. YH237 yhEx142[*nphp-1::cfp* + *che-13*::yfp + *rol-6(su1006)*] and MX254 Ex[*kap-1::gfp* + *rol-6(su1006)*] were used in ciliary localization studies. VC2695 *mapk-15(gk1234) III* was used in phenotypic assays, expression analysis, and genetic crosses. The following strains were generated as part of this study and are available upon request: LU517 *mapk-15(gk1234) III* 6X backcrossed to N2, LU518 and LU519 *mapk-15(gk1234) III*; *him-5(e1490) V*; lrEx179[*mapk-15(isoform A)::gfp* + *elt-2::mCherry* + pBlue], LU520 *mapk-15(gk1234) III*; *him-5(e1490) V*, LU527 and LU528 *mapk-15(gk1234) III*; lrEx187 [*mapk-15(isoform A)::gfp* + *elt-2::mCherry* + pBlue], LU529 and LU530 *mapk-15(gk1234) III*; lrEx188[*mapk-15(isoform C)::mCherry* + *elt-2::gfp* + pBlue], LU531 *mapk-15(gk1234) III*; *him-5(e1490) V*; lrEx187 [*mapk-15(isoform A)::gfp* + *elt-2::mCherry* + pBlue]; lrEx188[*mapk-15 (isoform C)::mCherry* + *elt-2::gfp* + pBlue], LU532 *mapk-15(gk1234) III*; *him-5(e1490) V*; myIs1[*pkd-2::gfp* + *unc-122p::gfp*] *IV*, LU534 *him-5 (el1490) V*; *daf-12(sa204) X*; lrEx190[*mapk-15p::mCherry*, *elt-2::gfp*; pBlue], LU535 *him-5(el1490) V*; *daf-12(sa204) X*; daf-19 (m86) *II*; lrEx190[*mapk-15p::mCherry* + *elt-2::gfp* + pBlue], LU536 *him-5(e1490) V*; lrEx188[*mapk-15(isoform C)::mCherry* + *elt-2::gfp* + pBlue], LU538 *mapk-15(gk1234) III*; *him-5(el1490) V*; lrEx190[*mapk-15p::mCherry* + *elt-2::gfp* + Pblue], LU539 *mapk-15(gk1234) III*; *him-5(e1490) V*; myIs1[*pkd-2::gfp* + *unc-122p::gfp*] *IV*, LU545 *mapk-15(gk1234) III*; *him-5(e1490) V*; lrEx194[*mapk-15(isoform A)::gfp* + *mapk-15(isoform C)::mCherry* + *elt-2::mCherry* + pBlue], LU548 lrEx193[*mapk-15p::mCherry* + pBlue]; yhEx142[*nphp-1::gfp* + *che-13::yfp* + *rol-6(su1006)*], LU550 *mapk-15*

(gk1234) III; *him-5(e1490) V*; yhEx142[*nphp-1::cfp* + *che-13::yfp* + *rol-6 (su1006)*], LU551 *mapk-15(gk1234) III*; *him-5(e1490) V*; lrEx193[*mapk-15p::mCherry* + pBlue]; yhEx142[*nphp-1::cfp* + *che-13::yfp* + *rol-6 (su1006)*], LU558 *mapk-15(gk1234)* III; lrEx188[*Pmapk-15::mapk-15(Isoform C)::mCherry* + *elt-2::gfp* + pBlue]; yhEx142[*nphp-1::cfp* + *che-13::yfp* + *rol-6(su1006)*], LU561 *him-5(e1490) V*; Ex[*kap-1::gfp* + *rol-6 (su1006)*]; lrEx188[*mapk-15(isoform C)::mCherry* + *elt-2::gfp* + pBlue], LU562 *him-5(e1490) V*; *mapk-15(gk1234) III*; lrEx196[*pkd-2p::mapk-15 (isoform A)::gfp* + elt-2::*mCherry* + pBlue].

4.3 | Phenotypic analysis

Dye-filling assays were performed using animals well fed for multiple generations by incubating them in 0.02 mg/ml DiI or DiO (Invitrogen, Carlsbad, CA, USA) in M9 buffer gently shaking for one hour at room temperature (Culotti and Russel, 1978; Perkins et al., 1986). Osmotic avoidance assays were performed by placing six animals in the center of a 60% glycerol ring, 3/8 inch in diameter on nematode growth media plates lacking food and observing them for eight minutes. The osmotic avoidance index is the proportion of animals remaining in the center after eight minutes (Culotti and Russel, 1978; Perkins et al., 1986). Male fertility assays were performed by examining the number of outcrossed progeny when five male worms were placed on a plate containing two L4 *dpy-17(e164)* hermaphrodites (Hodgkin, 1983). Male mating-response assays were performed as described previously (Barr and Sternberg, 1999; Bae, Kim, L'hernault, & Barr, 2009). The day before male mating response assays were performed, L4 males to be assayed were transferred to a separate plate. On the day of the experiment, ~3–5 males were transferred to a seeded plate containing ~30 *unc-31 (e169)* hermaphrodites and observed for 10 min. A positive response was scored when the male tail contacted and subsequently began scanning a hermaphrodite for at least 10 s within this 10-min period.

4.4 | Imaging

All strains were imaged using a Leica TCS SP5 II (Wetzlar, Germany) laser-scanning confocal microscope with a 40× (1.3 numeric aperture) or 63× (1.4 numeric aperture) oil-immersion lenses. Image acquisition and image processing was conducted using the Leica LAS software. Images were rotated and their brightness and contrast levels were adjusted using Adobe Photoshop (San Jose, CA). All images in Figures 2, 6, and 7 were obtained and adjusted using identical settings and values. Figures were prepared using Adobe Illustrator.

4.5 | Bioinformatics, domain, and statistical analyses

All DNA and protein sequences were obtained from www.wormbase.org (Harris et al., 2010). Sequence comparisons, including the identification of protein homologs were generated using a Basic Local Alignment Search Tool (Gish and States, 1993). The putative kinase domain was determined using InterProScan 5 (Jones et al., 2014). All statistical analyses were conducted using Microsoft Excel (Redmond, WA) and R studio (Boston, MA).

ACKNOWLEDGMENTS

This work was supported by a Major Research Instrumentation grant (MRI-1126711) from the National Science Foundation to BPP. The authors thank WormBase for computational resources and the National Bioresource Project for strains. Maureen Barr and Robert O'Hagan provided strains. Terese Swords and Eleanor Goblirsch provided assistance with genetics and strain maintenance. Louis Saldana assisted in PKD-2 experiments. An anonymous reviewer suggested analysis of the *mapk-15* transgene under control of the *pkd-2* promoter. Elizabeth De Stasio and Peter Swoboda provided insights and suggestions. Elizabeth De Stasio and Jan Burghoorn critically evaluated the manuscript.

REFERENCES

Avidor-Reiss, T., Maer, A. M., Koundakjian, E., Polyanovsky, A., Keil, T., Subramaniam, S., & Zuker, C. S. (2004). Decoding cilia function: Defining specialized genes required for compartmentalized cilia biogenesis. *Cell*, *117*, 527–39.

Bacallao, R. L., & McNeill, H. (2009). Cystic kidney diseases and planar cell polarity signaling. *Clinical Genetics*, *75*, 107–117.

Bae, Y. K., Kim, E., L'hernault, S. W., & Barr, M. M. (2009). The CIL-1 PI 5-phosphatase localizes TRP Polycystins to cilia and activates sperm in *C. elegans*. *Current Biology*, *19*, 1599–1607.

Barr, M. M., DeModena, J., Braun, D., Nguyen, C. Q., Hall, D. H., & Sternberg, P. W. (2001). The *Caenorhabditis elegans* autosomal dominant polycystic kidney disease gene homologs *lov-1* and *pkd-2* act in the same pathway. *Current Biology*, *11*, 1341–1346.

Barr, M. M., & Garcia, L. R. (2006). Male mating behavior. *WormBook*, 1–11.

Barr, M. M., & Sternberg, P. W. (1999). A polycystic kidney-disease gene homologue required for male mating behaviour in *C. elegans*. *Nature*, *401*, 386–389.

Blacque, O. E., Perens, E. A., Boroevich, K. A., Inglis, P. N., Li, C., Warner, A., ... Leroux, M. R. (2005). Functional genomics of the cilium, a sensory organelle. *Current Biology*, *15*, 935–41.

Brenner, S. (1974). The genetics of *Caenorhabditis elegans*. *Genetics*, *77*, 71–94.

Burghoorn, J., Piasecki, B. P., Crona, F., Phirke, P., Jeppsson, K. E., & Swoboda, P. (2012). The in vivo dissection of direct RFX-target gene promoters in *C. elegans* reveals a novel cis-regulatory element, the C-box. *Developmental Biology*, *368*, 415–426.

C. elegans Deletion Mutant Consortium. (2012). Large-scale screening for targeted knockouts in the Caenorhabditis elegans genome. *G3 (Bethesda)*, *2*, 1415–1425.

Cai, Y., Fedeles, S. V., Dong, K., Anyatonwu, G., Onoe, T., Mitobe, M., ... Somlo, S. (2014). Altered trafficking and stability of polycystins underlie polycystic kidney disease. *Journal of Clinical Investigation*, *124*, 5129–5144.

Chen, N., Mah, A., Blacque, O. E., Chu, J., Phgora, K., Bakhoum, M. W., ... Stein, L. D. (2006). Identification of ciliary and ciliopathy genes in *Caenorhabditis elegans* through comparative genomics. *Genome Biology*, *7*, R126.

Chia, J., Tham, K. M., Gill, D. J., Bard-Chapeau, E. A., & Bard, F. A. (2014). ERK8 is a negative regulator of O-GalNAc glycosylation and cell migration. *Elife*, *3*, e01828.

Chu, J. S., Tarailo-Graovac, M., Zhang, D., Wang, J., Uyar, B., Tu, D., ... Chen, N. (2012). Fine tuning of RFX/DAF-19-regulated target gene expression through binding to multiple sites in *Caenorhabditis elegans*. *Nucleic Acids Research*, *40*, 53–64.

Colecchia, D., Strambi, A., Sanzone, S., Iavarone, C., Rossi, M., Dall'Armi, C., … Chiariello, M. (2012). MAPK15/ERK8 stimulates autophagy by interacting with LC3 and GABARAP proteins. *Autophagy*, *8*, 1724–1740.

Culotti, J. G., & Russell, R L. (1978). Osmotic avoidance defective mutants of the nematode *Caenorhabditis elegans*. *Genetics*, *90*, 243–256.

Efimenko, E, Bubb, K., Mak, H. Y., Holzman, T., Leroux, M. R., Ruvkun, G., … Swoboda, P. (2005). Analysis of *xbx* genes in *C. elegans*. *Development*, *132*, 1923–1934.

Follit, J. A., San Agustin, J. T., Xu, F., Jonassen, J. A., Samtani, R., Lo, C. W., & Pazour, G. J. (2008). The Golgin GMAP210/TRIP11 anchors IFT20 to the Golgi complex. *PLoS Genetics*, *4*, e1000315.

Geng, L., Okuhara, D., Yu, Z., Tian, X., Cai, Y., Shibazaki, S., & Somlo, S. (2006). Polycystin-2 traffics to cilia independently of polycystin-1 by using an N-terminal RVxP motif. *Journal of Cell Science*, *119*, 1383–1395.

Gish, W., & States, D. J. (1993). Identification of protein coding regions by database similarity search. *Nature Genetics*, *3*, 266–272.

Harris, T. W., Antoshechkin, I., Bieri, T., Blasiar, D., Chan, J., Chen, W. J., … Sternberg, P. W. (2010). WormBase: A comprehensive resource for nematode research. *Nucleic Acids Research*, *38*, D463–467.

Henriksson, J., Piasecki, B. P., Lend, K., Burglin, T. R., & Swoboda, P. (2013). Finding ciliary genes: A computational approach. *Methods in Enzymology*, *525*, 327–350.

Hildebrandt, F., Benzing, T., & Katsanis, N. (2011). Ciliopathies. *New England Journal of Medicine*, *364*, 1533–1543.

Hodgkin, J. (1983). Male phenotypes and mating efficiency in *Caenorhabditis elegans*. *Genetics*, *103*, 43–64.

Hogan, M. C., Manganelli, L., Woollard, J. R., Masyuk, A. I., Masyuk, T. V., Tammachote, R., … Ward, C. J. (2009). Characterization of PKD protein-positive exosome-like vesicles. *Journal of the American Society of Nephrology*, *20*, 278–288.

Jones, P., Binns, D., Chang, H. Y., Fraser, M., Li, W., McAnulla, C., … Hunter, S. (2014). InterProScan 5: genome-scale protein function classification. *Bioinformatics*, *30*, 1236–1240.

Kim, H., Xu, H., Yao, Q., Li, W., Huang, Q., Outeda, P., … Qian, F. (2014). Ciliary membrane proteins traffic through the Golgi via a Rabep1/GGA1/Arl3-dependent mechanism. *Nature Communications* *5*:5482.

Kimura, Y., Kurabe, N., Ikegami, K., Tsutsumi, K., Konishi, Y., Kaplan, O. I., … Setou, M. (2010). Identification of tubulin deglutamylase among *Caenorhabditis elegans* and mammalian cytosolic carboxypeptidases (CCPs). *Journal of Biological Chemistry*, *285*, 22936–22941.

Li, J. B., Gerdes, J. M., Haycraft, C. J., Fan, Y., Teslovich, T. M., May-Simera, H., … Dutcher, S. K. (2004). Comparative genomics identifies a flagellar and basal body proteome that includes the BBS5 human disease gene. *Cell*, *117*, 541–552.

Maguire, J. E., Silva, M., Nguyen, K. C., Hellen, E., Kern, A. D., Hall, D. H., & Barr, M. M. (2015). Myristoylated CIL-7 regulates ciliary extracellular vesicle biogenesis. *Molecular Biology of the Cell*, *26*, 2823–2832.

Miyatake, K., Kusakabe, M., Takahashi, C., & Nishida, E. (2015). ERK7 regulates ciliogenesis by phosphorylating the actin regulator CapZIP in cooperation with Dishevelled. *Nature Communications*, *6*, 6666.

Mello, C., & Fire, A. (1995). DNA transformation. *Methods in Cell Biology*, *48*, 451–482.

O'Hagan, R., Piasecki, B. P., Silva, M., Phirke, P., Nguyen, K. C., Hall, D. H., … Barr, M. M. (2011). The tubulin deglutamylase CCPP-1 regulates the function and stability of sensory cilia in *C. elegans*. *Current Biology*, *21*, 1685–1694.

O'Hagan, R., Wang, J., & Barr, M. M. (2014). Mating behavior, male sensory cilia, and polycystins in *Caenorhabditis elegans*. *Seminars in Cell and Developmental Biology*, *33*, 25–33.

Pazour, G. J., Agrin, N., Leszyk, J., & Witman, G. B. (2005). Proteomic analysis of a eukaryotic cilium. *Journal of Cell Biology*, *170*, 103–113.

Pazour, G. J., & Bloodgood, R. A. (2008). Targeting proteins to the ciliary membrane. *Current Topics in Developmental Biology*, *85*, 115–149.

Pazour, G. J., San Agustin, J. T., Follit, J. A., Rosenbaum, J. L., & Witman, G. B. (2002). Polycystin-2 localizes to kidney cilia and the ciliary level is elevated in orpk mice with polycystic kidney disease. *Current Biology*, *12*, R378–380.

Peden, E. M., & Barr, M. M. (2005). The KLP-6 kinesin is required for male mating behaviors and polycystin localization in *Caenorhabditis elegans*. *Current Biology*, *15*, 394–404.

Perkins, L. A., Hedgecock, E. M., Thomson, J. N., & Culotti, J. G. (1986). Mutant sensory cilia in the nematode *Caenorhabditis elegans*. *Developmental Biology*, *117*, 456–487.

Piasecki, B. P., Burghoorn, J., & Swoboda, P. (2010). Regulatory Factor X (RFX)-mediated transcriptional rewiring of ciliary genes in animals. *Proceedings of the National Academy of Sciences of the United States of America*, *107*, 12969–12974.

Pisitkun, T., Shen, R. F., & Knepper, M. A. (2004). Identification and proteomic profiling of exosomes in human urine. *Proceedings of the National Academy of Sciences of the United States of America*, *101*, 13368–13373.

Rossi, M., Colecchia, D., Ilardi, G., Acunzo, M., Nigita, G., Sasdelli, F., … Chiariello, M. (2016). MAPK15 upregulation promotes cell proliferation and prevents DNA damage in male germ cell tumors. *Oncotarget*, *7*, 20981–20998.

Satir, P., & Christensen, S. T. (2008). Structure and function of mammalian cilia. *Histochemistry and Cell Biology*, *129*, 687–693.

Scheffers, M. S., Le, H., van der Bent, P., Leonhard, W., Prins, F., Spruit, L., … Peters, D. J. (2002). Distinct subcellular expression of endogenous polycystin-2 in the plasma membrane and Golgi apparatus of MDCK cells. *Human Molecular Genetics*, *11*, 59–67.

Schouteden, C., Serwas, D., Palfy, M., & Dammermann, A. (2015). The ciliary transition zone functions in cell adhesion but is dispensable for axoneme assembly in *C. elegans*. *Journal of Cell Biology*, *210*, 35–44.

Starich, T. A., Herman, R. K., Kari, C. K., Yeh, W. H., Schackwitz, W. S., Schuyler, M. W., … Riddle, D. L. (1995). Mutations affecting the chemosensory neurons of *Caenorhabditis elegans*. *Genetics*, *139*, 171–188.

Su, X., Driscoll, K., Yao, G., Raed, A., Wu, M., Beales, P. L., & Zhou, J. (2014). Bardet-Biedl syndrome proteins 1 and 3 regulate the ciliary trafficking of polycystic kidney disease 1 protein. *Human Molecular Genetics*, *23*, 5441–5451.

Sulston, J. E., Albertson, D. G., & Thomson, J. N. (1980). The *Caenorhabditis elegans* male: postembryonic development of nongonadal structures. *Developmental Biology*, *78*, 542–576.

Swoboda, P., Adler, H. T., & Thomas, J. H. (2000). The RFX-type transcription factor DAF-19 regulates sensory neuron cilium formation in *C. elegans*. *Molecular Cell*, *5*, 411–421.

Wang, J., & Barr, M. M. (2016). Ciliary extracellular vesicles: Txt msg organelles. *Cellular and Molecular Neurobiology*, *36*, 449–457.

Wang, J., Kaletsky, R., Silva, M., Williams, A., Haas, L. A., Androwski, R. J., … Barr, M. M. (2015). Cell-specific transcriptional profiling of ciliated sensory neurons reveals regulators of behavior and extracellular vesicle biogenesis. *Current Biology*, *25*, 3232–3238.

Wang, J., Schwartz, H. T., & Barr, M. M. (2010). Functional specialization of sensory cilia by an RFX transcription factor isoform. *Genetics*, *186*, 1295–1307.

Wang, J., Silva, M., Haas, L. A., Morsci, N. S., Nguyen, K. C., Hall, D. H., & Barr, M. M. (2014). *C. elegans* ciliated sensory neurons release extracellular vesicles that function in animal communication. *Current Biology*, *24*, 519–525.

Ward, H. H., Brown-Glaberman, U., Wang, J., Morita, Y., Alper, S. L., Bedrick, E. J., … Wandinger-Ness, A. (2011). A conserved signal and GTPase complex are required for the ciliary transport of polycystin-1. *Molecular Biology of the Cell*, *22*, 3289–3305.

Williams, C. L., Li, C., Kida, K., Inglis, P. N., Mohan, S., Semenec, L., … Leroux, M. R. (2011). MKS and NPHP modules cooperate to establish basal body/transition zone membrane associations and ciliary gate function during ciliogenesis. *Journal of Cell Biology*, *192*, 1023–1041.

Williams, C. L., Winkelbauer, M. E., Schafer, J. C., Michaud, E. J., & Yoder, B. K. (2008). Functional redundancy of the B9 proteins and nephrocystins in *Caenorhabditis elegans* ciliogenesis. *Molecular Biology of the Cell*, *19*, 2154–2168.

Wood, C. R., Huang, K., Diener, D. R., & Rosenbaum, J. L. (2013). The cilium secretes bioactive ectosomes. *Current Biology*, *23*, 906–911.

Xu, Q., Zhang, Y., Wei, Q., Huang, Y., Li, Y., Ling, K., & Hu, J. (2015). BBS4 and BBS5 show functional redundancy in the BBSome to regulate the degradative sorting of ciliary sensory receptors. *Science Reports*, *5*, 11855.

Yoder, B. K., Hou, X., & Guay, W. L. M. (2002). The polycystic kidney disease proteins, polycystin-1, polycystin-2, polaris, and cystin, are co-localized in renal cilia. *Journal of the American Society of Nephrology*, *13*, 2508–2516.

SUPPORTING INFORMATION

Additional Supporting Information may be found online in the supporting information tab for this article.

How to cite this article: Piasecki BP, Sasani TA, Lessenger AT, Huth N, Farrell S. MAPK-15 is a ciliary protein required for PKD-2 localization and male mating behavior in *Caenorhabditis elegans*. *Cytoskeleton*. 2017;74:390–402. https://doi.org/10.1002/cm.21387